

# Magnetoresistance Amplification Effect in Silicon Transistor Device

Tao Wang, Dezheng Yang,\* Mingsu Si, Fangcong Wang, Shiming Zhou, and Desheng Xue\*

Large magnetoresistance discovered in nonmagnetic semiconductors offers an alternative route to renew magnetoelectronics without ferromagnets. However, it is still a great challenge to retain such large magnetoresistance under low magnetic fields. In this work, analogous to current amplification in the transistor, a magnetoresistance amplification effect is proposed in silicon transistor device, where the device current is significantly controlled by magnetic-field-manipulated coupling of two  $p$ - $n$  junctions in transistor. As a direct consequence, large magnetoresistance of 50 000% with high sensitivity of 50%  $\text{Oe}^{-1}$  is yielded at magnetic field of only 0.1 T. The results not only provide here a new proposal compatible with current semiconductor technology to achieve large magnetoresistance at low magnetic field, but also realize magnetic-field-manipulated transistor, which is a step for magnetoelectronics.

## 1. Introduction

Combining magnetic functionality with semiconductor technology remains a challenging task in semiconductor magnetoelectronics, both because of the material constraints and the low spin injection efficiency from ferromagnet into semiconductor.<sup>[1,2]</sup> Recently, the discovery of large magnetoresistance (MR) in conventional semiconductors, even larger than magnetic materials, offers an alternative route to renew magnetoelectronics without any ferromagnet.<sup>[3–12]</sup> Unlike the negligible ordinary MR in semiconductors, where the magnetic field effect was almost compensated by spontaneous Hall electric field, experiments and theories both proposed that the inhomogeneity can elegantly solve that problem to obtain such unexpected large MR effect in semiconductor.<sup>[3–15]</sup> For example, the inhomogeneity has been successfully introduced by random

impurity-doping in  $\text{Ag}_2\text{Te/Se}$ ,<sup>[3,4]</sup> deflected current path in inhomogeneous InSb disk,<sup>[5]</sup> and nonuniform electric field distribution in Si.<sup>[8–11]</sup>

According to this concept, the conventional  $p$ - $n$  junction device (or Schottky junction) can also be reviewed as a novel platform to obtain large MR,<sup>[16–20]</sup> which naturally has an electric field inhomogeneity at the junction interface, also known as the space charge region.<sup>[21]</sup> With increasing the magnetic fields to modify the space charge region, the turn-on voltage of  $p$ - $n$  junction significantly increases, yields a large positive MR. However, from the view of the development of electronics, the devices performed in our daily life only consist with a few basic building blocks i.e. diode and transistor.

Therefore, the next challenge for semiconductor magnetoelectronics is to go beyond large MR to build its own basic building blocks for the specified magnetic functionality.<sup>[22–24]</sup>

Our work aims to address this challenge by proposing MR amplification effect in a silicon transistor. Analogous to the well-known electric amplification effect of a transistor,<sup>[21]</sup> we realize MR amplification in the silicon  $p^+n$ - $n^+$  device, where the coupling strength between the  $\text{Si}(p^+)$ - $\text{Si}(n)$  and  $\text{Si}(n)$ - $\text{Si}(n^+)$  junctions is controlled by magnetic field. When the coupling between two  $p$ - $n$  junctions was formed, a signature negative differential resistance was observed in the voltage and current characteristics, which strongly enhances both the MR and the magnetic sensitivity of silicon transistor. As direct evidence, at temperature of 10 K and magnetic field of only 0.1 T, MR in silicon transistor is amplified up to 50 000% and the magnetic field sensitivity is enhanced as high as 50%  $\text{Oe}^{-1}$ , which is three orders of magnitude larger than that of reported Si semiconductor electronics.<sup>[8–11]</sup> Our result not only reveals a new proposal to achieve a large MR at low magnetic field for semiconductor device, but also provides a novel prototype of magnetic transistor in magnetoelectronics. As one of the most fundamental elements of modern electronics, transistor endowed with such innovative capabilities will invigorate future semiconductor research.

## 2. Experiment Results

To compatible with the conventional semiconductor technology, we fabricated transistor by implanting boron and

T. Wang, Dr. D. Z. Yang, Dr. M. S. Si,  
Dr. F. C. Wang, Prof. D. S. Xue  
Key Laboratory for Magnetism and  
Magnetic materials of Ministry of Education  
Lanzhou University  
Lanzhou 730000, China  
E-mail: yangdzh@lzu.edu.cn; xueds@lzu.edu.cn  
Prof. S. M. Zhou  
Department of Physics  
Tongji University  
Shanghai 200092, China



DOI: 10.1002/aelm.201600174

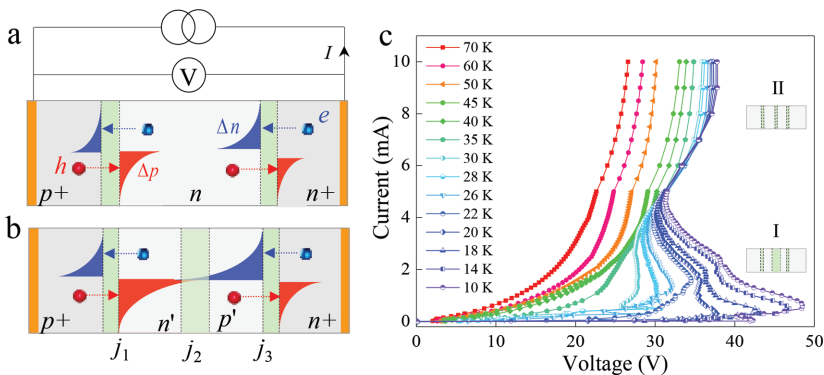


**Figure 1.** a) Schematic illustration of the magnetic transistor device structure and measurement sketch. The light green regions represent the space-charge regions. At high temperature, the two  $p$ - $n$  junctions are uncoupled. b) The sketch of the coupled transistor at low temperature. When injection carriers from  $n^+$  and  $p^+$  into the  $n$  region overlap each other, which induces the coupling of two  $p$ - $n$  junctions, a new space-charge region  $j_2$  is formed. c) A transition from diode-like to thyristor-like  $I$ - $V$  curves occurs with decreasing the temperature under magnetic field 2 T, indicating the coupling of two  $p$ - $n$  junctions. The insets in Figure b show two bistable states of thyristor: the forward blocking mode (I) and the forward conducting mode (II).

phosphorus ions at the top and bottom surfaces of silicon, respectively. The Cu electrodes were sputtered at both surfaces of silicon. The device size is  $3 \text{ mm} \times 3 \text{ mm} \times 0.5 \text{ mm}$ . **Figure 1a** shows the measurement diagram as well as the device schematic. During the measurement the current is applied from  $p^+$  region to  $n^+$  region and magnetic field was perpendicular to the current and parallel to the sample plane. According to the doping, the silicon device is separated into three regions:  $\text{Si}(p^+)$ ,  $\text{Si}(n)$ , and  $\text{Si}(n^+)$ . The corresponding carrier densities are  $2.0 \times 10^{14}$ ,  $1.0 \times 10^{12}$ , and  $1.0 \times 10^{15} \text{ cm}^{-3}$ , respectively. Due to the different carrier concentrations,  $p^+$ - $n$  and  $n$ - $n^+$  junction, namely,  $\text{Si}(p^+)/\text{Si}(n)$  and  $\text{Si}(n)/\text{Si}(n^+)$ , are formed. Compared to previous magnetodiode,<sup>[25–29]</sup> such device layout features the coupling of these two  $p$ - $n$  junctions. By adjusting temperature to change the carrier diffusion length  $l$ , we can tune the states of coupling of transistor. When  $l$  is less than the width of  $n$  region ( $\approx 500 \text{ }\mu\text{m}$ ) in our device at room temperature,<sup>[30]</sup> the two  $p$ - $n$  junctions can be considered as two individual  $p$ - $n$  junctions in series (Figure 1a). However, with decreasing temperature,  $l$  increases and becomes comparable to the width of  $n$  region. In this situation, the two  $p$ - $n$  junctions are coupled due to the overlap of injected carriers in the  $n$  region. As shown in Figure 1b, the two  $p$ - $n$  junctions form a coupled  $p^+n'-p'n^+$  transistor, and the new coupled region  $j_2$  is generated.

In order to confirm the above scenario for the coupling of two  $p$ - $n$  junctions in silicon transistor device, the  $I$ - $V$  characteristics with various temperatures are displayed in Figure 1c. Clearly, in our devices, two types of temperature-dependent  $I$ - $V$  characteristics are observed, indicating the occurrence of the coupling in these two  $p$ - $n$  junctions. For  $T > 40 \text{ K}$ , the current increases exponentially with the voltage. This is a typical diode-like feature, where the device is conducting at positive voltage. While, below 40 K the device is still blocked at positive voltages at the beginning. As the voltage increases to a critical value  $V_p$  (around at  $I = 1 \text{ mA}$ ), the blocking state is changed and a sharp negative differential resistance for a wide current range from

1 to 5 mA is observed. When the current is further beyond 5 mA, the  $I$ - $V$  curves return back to the exponential relationship, similar to those curves at  $T > 40 \text{ K}$ . Interestingly, such peculiar  $I$ - $V$  characteristic below 40 K is insightfully the same as that of thyristor,<sup>[31,32]</sup> which is usually considered as a coupled transistor. In contrast with diode-like feature only with one conducting state in the positive voltage, for thyristor-like feature there are two distinct states in the positive voltage range, usually defined as the forward blocking state and the forward conducting state. As shown in inset I of Figure 1c, the forward blocking state originates from the reverse biased  $j_2$  at the positive voltage, regardless of the forward biased  $j_1$  and  $j_3$ , while the forward conducting state (inset II) is formed by the breakdown of the reverse biased junction  $j_2$  under the larger positive voltage. Moreover, we also measured the  $I$ - $V$  curves of transistor device by using the voltage source to double-check the coupling of two  $p$ - $n$  junctions. Interestingly, we observed a sudden

jump when the voltage bias reaches to the critical  $V_p$  (Figure S1, Supporting Information), instead of the negative differential resistance when using the current source.

Because the total current for the transistor is mainly contributed by the diffusion of the minority carrier, even if the concentration of the minority carrier is very small.<sup>[31]</sup> Therefore, we only discussed the temperature dependent of the transport of diffused minority carriers, which controls the current of the whole device. As we know, the minority carrier diffusion length is the average distance the minority carrier can move. It is related to the carrier lifetime  $\tau$  and the carrier mobility  $\mu$ , according to the following formula:  $l = (\mu k T \tau / q)^{1/2}$ . Although minority carrier life time slightly decreases with temperature, the minority carrier mobility increases more sharply with decreasing temperature, especially below 50 K. As a result, the minority carrier diffusion length  $l$  is expected to increase with the decrease of the temperature. In silicon, at 300 K the lifetime can be estimated 0.1 ms, and the minority carrier mobility is  $\mu = 480 \text{ cm}^2 \text{ V}^{-1} \text{ s}^{-1}$ , thus  $l$  is about 354  $\mu\text{m}$ , which is consistent with the previous experiment.<sup>[30,33–36]</sup> At 40 K, the lifetime and the minority carrier mobility are 0.03 ms and  $2.2 \times 10^4 \text{ cm}^2 \text{ V}^{-1} \text{ s}^{-1}$ , respectively. Thus,  $l$  is about 500  $\mu\text{m}$ , which is quite close to the  $n$  region of our device. As a result, the two  $p$ - $n$  junction can be considered as coupling below 40 K, as shown in Figure 1b.

As a typical nonlinear electric device, thyristor can be switched between these two different conductance states. However, it is usually triggered by external electric field.<sup>[31,32]</sup> In **Figure 2** we show that the bistable resistance in thyristor can be manipulated by magnetic field, which induces a significant MR amplification effect. In order to demonstrate such MR amplification effect, we compare the  $I$ - $V$  characteristics manipulated by magnetic field with uncoupled and coupled transistors. For the uncoupled transistor with diode-like feature, the current starts to be suppressed until magnetic field increases to several teslas (Figure 2a). This will yield a large MR but a

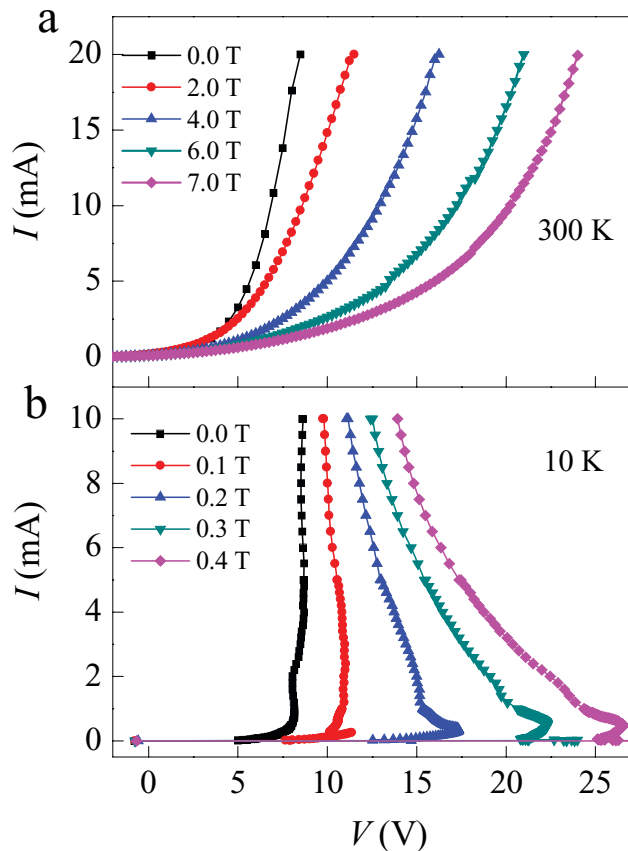


**Figure 2.** a) The diode-like  $I$ - $V$  curves at  $T = 300$  K are manipulated by large magnetic fields from 0 to 7 T, demonstrating uncoupled transistor manipulated by the magnetic field. b) The thyristor-like  $I$ - $V$  curves at  $T = 10$  K are tuned by small magnetic fields only from 0 to 0.4 T, demonstrating the coupled transistor manipulated by magnetic field.

low magnetic sensitivity ( $S$ ).<sup>[16–18]</sup> For instance, under large magnetic field amplitude of 7 T, MR is about 1400% at voltage bias 8.5 V, but  $S$  is only 0.02%  $\text{Oe}^{-1}$ . Here MR is defined as  $\text{MR}(\%) = [R(H) - R(0)]/R(0) \times 100\%$  with  $R(0)$  and  $R(H)$  being the resistances ( $V/I$ ) at the magnetic fields zero and  $H$ , respectively, and magnetic sensitivity  $S$  is calculated by  $S = \text{MR}(\%)/H$ . However, for the coupled transistor with thyristor-like feature, the critical voltage  $V_p$  is very sensitive to the magnetic field shown in Figure 2b, which works in the same way as a conventional thyristor if we applied electric field to replace the magnetic field.<sup>[31]</sup> With applying a low magnetic field only from 0 to 0.4 T,  $V_p$  significantly increases from 5 to 26 V. Interestingly, when  $V_p$  is larger than the applied bias voltage, the device can be switched from the forward conducting state to the blocking state. As a typical feature of MR amplification, this behavior acts like a magnetic switch that causes an extremely large MR and high sensitivity  $S$ . For example, at the same bias voltage 8.5 V and applying a magnetic field of only 0.1 T to switch the bistable states, MR is up to 50 000%, and  $S$  is as high as 50%  $\text{Oe}^{-1}$ , which is even larger than that of nowadays commercial magnetic sensors.<sup>[37]</sup> Remarkably, at larger current level, i.e.,  $I = 10$  mA one can find that the transistor becomes insensitive to low magnetic field, indicating that the MR amplification

effect disappears. This is because that the coupled region  $j_2$  is broken at the higher electric field. The result also confirms that the coupling of two  $p$ - $n$  junctions plays a key role for the MR amplification effect. In Figure S2 in the Supporting Information, we also show that for using voltage source, the  $V_p$  of thyristor is also sensitive to magnetic field.

Obviously, comparing our devices with the traditional magnetodiode<sup>[25–29]</sup> and magnetic transistor,<sup>[38,39]</sup> our devices have different  $I$ - $V$  characteristics and MR mechanisms. In our device the large MR effect stems from the change of the space-charge region  $j_2$  induced by magnetic field. However, the magnetodiode effect is based on the different combinations of carriers at the high and low recombining surfaces under the magnetic field, thus induced the concentration change.<sup>[25–29]</sup> The previous magnetic transistor devices are explained by only plasma deflections under magnetic field.<sup>[38,39]</sup> More importantly, according to our model, the key of MR amplification effect is that the minority carrier diffusion length should be comparable to the width of the  $n$  region. If such condition can be satisfied at room temperature, a significant room temperature MR amplification effect should be observed. We could use two methods to enhance the device working temperature. One is to decrease the width of the  $n$  region of the transistor. The other method is to enhance the minority carrier diffusion length by optimizing the fabrication process or using the semiconductor with the long minority carrier diffusion length. Moreover, based on this model, the semiconductor device with the negative differential resistance at room temperature could also be a very promising candidate for the MR amplification effect.

Although the increase of carrier mobility with decreasing temperature can also enhance MR, it is not the reason to contribute the MR amplification effect. Figure 3a shows transistor voltages as a function of temperature in the magnetic field range from 0 to 5 T. The current was selected to be 1 mA, at which the device just works at the critical voltage  $V_p$ . It is seen that an obvious kink appears at near 40 K, which is consistent with the Figure 1c. For temperature range above 40 K, the measured voltages increase only under the high magnetic field, i.e.,  $H > 1$  T, whereas, for temperature range below 40 K, the measured voltages significantly increase under the low magnetic field. Considering the continuity of carrier mobility with decreasing temperature, this kink can rule out that the MR amplification effect is caused by the increase of carrier mobility. The more detailed data are measured and shown in Figure S3 in the Supporting Information. Moreover, the occurrence of the kink in the  $V$ - $T$  curves also indicates the different MR behaviors for uncoupled and coupled transistors.

Figure 3b shows the typical MR curves for coupled and uncoupled transistors with the current ranging from 1 to 10 mA. In order to confirm that the MR amplification effect can occur at the low magnetic field, we also measured the MR performance at lower magnetic field from  $-0.1$  to  $0.1$  T, as shown in Figure S4 of the Supporting Information. One can easily find that MR for  $I = 1$  mA contrasts to other currents. For  $I = 1$  mA, MR of coupled transistor sharply increases at the low magnetic field and then saturates beyond 2.5 T. While, for the current is ranging from 3 to 9 mA, MR is smaller than that of coupled transistor at the low magnetic field, but is unsaturated even at a large magnetic field of 5 T, which is consistent with that

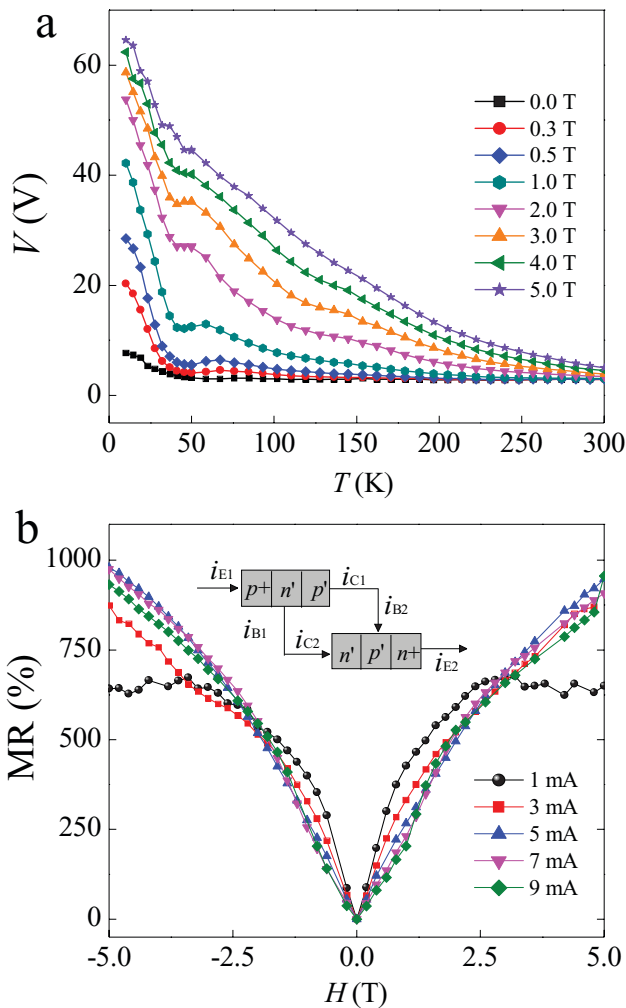


**Figure 3.** a) The transistor voltage at  $I = 1$  mA as a function of temperature. An obvious kink at  $T = 40$  K separates the coupled and uncoupled transistors under the magnetic fields from 0 to 5 T. b) Two types of MR for coupled and uncoupled transistors at  $T = 20$  K. By utilizing the amplification effect of transistor, the magnetic field sensitivity is significantly enhanced at small magnetic field. The inset demonstrates that the coupling of two  $p$ - $n$  junctions can be considered as the analogy of two-coupled transistor.

of Si device reported before.<sup>[6–12]</sup> Here we mainly focus on the MR amplification effect in the coupled transistor, which can be described by a schematic model of two-coupled transistor.<sup>[31]</sup> As illustrated in the inset of Figure 3b, we shows that the two transistors have a common  $n'$ - $p'$  region in order to represent the coupled transistor. This means that  $i_{B1} = i_{C2}$ ,  $i_{C1} = i_{B2}$ , and  $i_{E1} = i_{E2}$ , where the  $i_B$ ,  $i_C$ , and  $i_E$  are the currents through the base, collector, and emitter regions, respectively. If we associate current transfer ratio from an emitter to the collector  $\alpha$  with each transistor, we can solve the current  $i$  of two-coupled transistor as  $i = \frac{I_{CO1} + I_{CO2}}{1 - (\alpha_1 + \alpha_2)}$ , where  $I_{CO}$  is the collector saturation current. When the space charge region  $j_2$  is formed due to the coupling, this corresponds to very small  $\alpha_1$  and  $\alpha_2$ . In this case, the obtained current  $i$  through the device is approximately equal to  $I_{CO1} + I_{CO2}$  and the device is working in the forward blocking

state. However, as the breakdown of space-charge region  $j_2$  under the critical voltage  $V_p$ ,  $\alpha_1 + \alpha_2$  is close to 1 and the current sharply increases. In this situation, the device is switched to the forward conducting mode.

Importantly, in our work the current transfer ratio  $\alpha$  of transistor is manipulated by magnetic field, which induces the MR amplification. In order to clarify this, we compare the MR amplification effect to the electric amplification effect in Figure 4. For electric amplification effect of the vacuum tube, the grid under electric field controls the flow of thermionic electrons from cathode to anode, thus tune the current transfer ratio (Figure 4a). In 1940s, the idea of electric amplification effect in the vacuum tube was transferred to  $p$ - $n$  junction transistor by Shockley.<sup>[40]</sup> While, for magnetic amplification effect, the coupling region  $j_2$  between two  $p$ - $n$  junctions just likes the grid in a vacuum tube. Applying the magnetic field changes the coupling region and also controls carriers to flow it (Figure 4b). When the magnetic field is applied, the carriers in the  $n$ -type and  $p$ -type regions are deflected by the Lorentz force and accumulate at the edges of the sample (Figure 4b). As a result, a trapezoidal distribution in the space charge region is formed to balance the Lorentz force. Therefore, similar to the rectifying effect under the electric field, the spatial distribution in the space charge region under the external magnetic field can also drastically affect the junction resistance. Because our sample can be considered as the analogy of two-coupled transistors, we

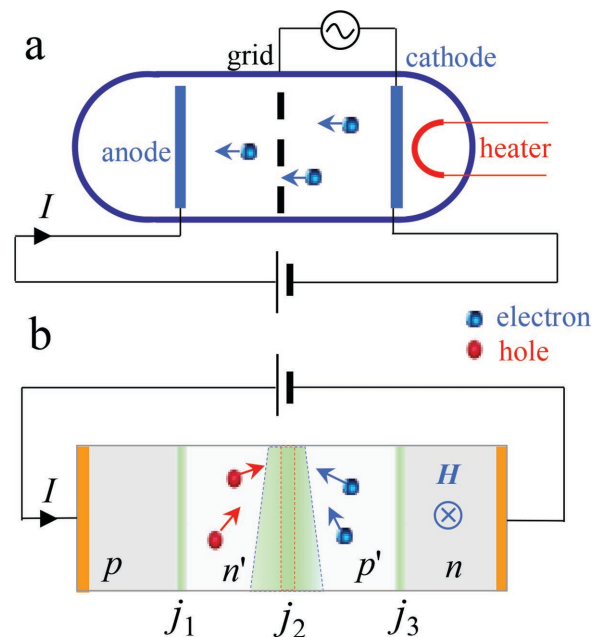


**Figure 4.** a) Illustration of the electric amplification effect based on a vacuum tube, the first electronic amplifying device. Thermionic electrons emitted by the cathode travel through the tube and are collected by the anode. Adding control grid within the tube allows the current between the cathode and the anode to be manipulated by the voltage on the grid. b) Illustration of the MR amplification effect. The magnetic transistor device we proposed closely corresponds to the vacuum tube: the collector region  $j_1$  to the anode, the coupling region  $j_2$  to the grid wires, and the emitter region  $j_3$  to the cathode. Applying a magnetic field changes the coupling region of transistor and controls the current through it.

can analyze the magnetic-field-modulated current transfer ratio of the device by transistor model.<sup>[30,34]</sup> For a transistor, the total current  $I$  can be described by  $I = qA \frac{D_p}{L_p} \left( \Delta p_E \operatorname{csch} \frac{W_b}{L_p} \right)$  where  $q$ ,  $A$ ,  $D_p$ ,  $L_p$ ,  $\Delta p_E$ , and  $W_b$  are electron charge, area of the junction, hole diffusion constant, hole diffusion length, excess hole concentration at the edge of emitter, and the width of base region, respectively. According to the above current model of transistor, the magnetic-field-manipulated coupling directly induced the current change based on two reasons. One is that the injection carrier concentration from two  $p$ - $n$  junctions is significantly controlled by magnetic field. Here we consider the influence of magnetic field as the first-order of perturbation of the width of base region. Because for  $p$ - $n$  junctions the current is exponential to the voltage due to the change of the width of base region, the excess hole concentration at the edge of space charge region modulated by applied magnetic field can be described by  $\Delta p_E(H) = \Delta p_E e^{-z_1 |H|}$ , where  $z_1$  is scale factor.<sup>[36]</sup> The other one is that the width of the coupled region  $j_2$  is manipulated by magnetic field. As a first-order perturbation, the width change can be directly described by the following relationship:  $W_b = W_{b0}(1 - z_2 |H|)$ , where  $z_2$  is the scale factor with respect to the base region width. Therefore, we can obtain the current manipulated by magnetic field as  $I = qA \frac{D_p}{L_p} \left( \Delta p_E e^{-z_1 |H|} \operatorname{csch} \frac{W_b(1 - z_2 |H|)}{L_p} \right)$ . The calculated current transfer ratio and MR were shown in Figure S5 of the Supporting Information, which were similar with our experimental results. Because the mechanism in our device is the same with the conventional electronics by utilizing the space charge region, we believe the new magnetoelectronics device with more complex functions will be designed based on the prototype of our magnetic transistor in future.

### 3. Conclusion

In summary, we proposed and realized a silicon transistor to amplify the MR of semiconductor device. A peculiar thyristor-like characteristic is observed in the coupled transistor, accompanied with a signature negative differential resistance. When the current transfer of transistor  $\alpha$  is tuned by magnetic field, the device can be switched between two bistable states by magnetic field, which works the same way as the conventional thyristor switched by electric field. As a direct consequence, both MR and field sensitivity  $S$  of the device can be amplified to 50 000% and 50%  $\text{Oe}^{-1}$ , respectively. Since our results have realized the large magnetoelectronics feature of  $p$ - $n$  junction, it should bring more tantalizing prospect of incorporating magnetic, optical and electronic functionality together within a monolithic semiconductor device, by combination of excellent optoelectronic feature of  $p$ - $n$  junction.

### Supporting Information

Supporting Information is available from the Wiley Online Library or from the author.

### Acknowledgements

This work was supported by National Basic Research Program of China (Grant No. 2012CB933101), the NSFC of China (Grant No. 51372107), and the PCSIRT (Grant No. IRT1251).

Received: April 28, 2016

Revised: June 26, 2016

Published online:

- [1] H. Ohno, *Science* **2001**, 291, 840.
- [2] I. Zutic, J. Fabian, S. Das Sarma, *Rev. Mod. Phys.* **2004**, 76, 323.
- [3] R. Xu, A. Husmann, T. F. Rosenbaum, M. L. Saboungi, J. E. Enderby, P. B. Littlewood, *Nature* **1997**, 390, 57.
- [4] J. S. Hu, T. F. Rosenbaum, J. B. Betts, *Phys. Rev. Lett.* **2005**, 95, 186603.
- [5] S. A. Solin, T. Thio, D. R. Hines, J. J. Heremans, *Science* **2000**, 289, 1530.
- [6] J. J. H. M. Schoonus, F. L. Bloom, W. Wagemans, H. J. M. Swagten, B. Koopmans, *Phys. Rev. Lett.* **2008**, 100, 127202.
- [7] J. J. H. M. Schoonus, P. P. J. Haazen, H. J. M. Swagten, B. Koopmans, *J. Phys. D: Appl. Phys.* **2009**, 42, 185011.
- [8] M. P. Delmo, S. Yamamoto, S. Kasai, T. Ono, K. Kobayashi, *Nature* **2009**, 457, 1112.
- [9] M. P. Delmo, E. Shikoh, T. Shinjo, M. Shiraishi, *Phys. Rev. B* **2013**, 87, 245301.
- [10] C. Wan, X. Zhang, X. Gao, J. Wang, X. Tan, *Nature* **2011**, 477, 304.
- [11] C. H. Wan, Z. H. Yuan, P. Liu, H. Wu, P. Guo, D. L. Li, S. S. Ali, *Appl. Phys. Lett.* **2013**, 103, 262406.
- [12] N. A. Porter, C. H. Marrows, *Sci. Rep.* **2012**, 2, 565.
- [13] M. M. Parish, P. B. Littlewood, *Nature* **2003**, 426, 162.
- [14] M. M. Parish, P. B. Littlewood, *Phys. Rev. B* **2005**, 72, 094417.
- [15] V. Guttal, D. Stroud, *Phys. Rev. B* **2005**, 71, 201304.
- [16] D. Z. Yang, F. C. Wang, Y. Ren, Y. L. Zuo, Y. Peng, S. M. Zhou, D. S. Xue, *Adv. Funct. Mater.* **2013**, 23, 2918.
- [17] T. Wang, M. S. Si, D. Z. Yang, Z. Shi, F. C. Wang, Z. L. Yang, S. M. Zhou, D. X. Xue, *Nanoscale* **2014**, 6, 3978.
- [18] D. Z. Yang, T. Wang, W. B. Sui, M. S. Si, D. W. Guo, Z. Shi, F. C. Wang, D. S. Xue, *Sci. Rep.* **2015**, 5, 11096.
- [19] Z. G. Sun, M. Mizuguchi, T. Manago, H. Akinaga, *Appl. Phys. Lett.* **2004**, 85, 5643.
- [20] K. Zhang, H. H. Li, P. Grunberg, Q. Li, S. T. Ye, Y. F. Tian, S. S. Yan, Z. J. Lin, S. S. Kang, Y. X. Chen, G. L. Liu, L. M. Mei, *Sci. Rep.* **2015**, 5, 14249.
- [21] W. Shockley, *Bell Syst. Tech. J.* **1949**, 28, 435.
- [22] S. Joo, T. Kim, S. H. Shin, J. Y. Lim, J. Hong, J. D. Song, J. Chang, H. W. Lee, K. Rhie, S. H. Han, K. H. Shin, M. Johnson, *Nature* **2013**, 494, 72.
- [23] S. H. Wang, W. X. Wang, L. K. Zou, X. Zhang, J. W. Cai, Z. G. Sun, B. G. Shen, J. R. Sun, *Adv. Mater.* **2014**, 26, 8059.
- [24] Z. C. Luo, X. Z. Zhang, C. Y. Xiong, J. J. Chen, *Adv. Funct. Mater.* **2015**, 25, 158.
- [25] E. I. Karakushan, V. I. Stafeev, *Sov. Phys. Solid State* **1961**, 3, 493.
- [26] H. Pfeleiderer, *Solid-State Electron.* **1972**, 15, 335.
- [27] G. A. Egiazaran, G. A. Mnatsakanyan, V. I. Murygin, V. I. Stafeev, *Sov. Phys. Semicond.* **1976**, 9, 829.
- [28] M. S. Cristoloveanu, J. De Poncharra, *IEEE Trans. Electron. Devices* **1981**, 28, 237.
- [29] F. J. Morin, J. P. Maita, *Phys. Rev.* **1954**, 28, 96.
- [30] T. Fuyuki, H. Kondo, T. Yamazaki, Y. Takahashi, Y. Uraoka, *Appl. Phys. Lett.* **2005**, 86, 262108.
- [31] B. G. Streetman, S. K. Banerjee, *Solid State Electronic Devices*, 6th ed., Prentice-Hall, Englewood Cliffs, NJ **1980**.

- [32] F. Sawano, I. Terasaki, H. Mori, T. Mori, M. Watanabe, N. Ikeda, Y. Nogami, Y. Noda, *Nature* **2005**, *437*, 522.
- [33] C. H. Wang, K. Misiakos, A. Neugroschel, *Appl. Phys. Lett.* **1989**, *54*, 2233.
- [34] C. H. Wang, K. Misiakos, A. Neugroschel, *Appl. Phys. Lett.* **1990**, *57*, 159.
- [35] D. B. M. Klaassen, *Solid-State Electron.* **1992**, *35*, 961.
- [36] J. Linnros, V. V. Grivickas, *Phys. Rev. B* **1995**, *50*, 16943.
- [37] S. A. Wolf, D. D. Awschalom, R. A. Buhrman, J. M. Daughton, S. von Molnar, M. L. Roukes, A. Y. Chtchelkanova, D. M. Treger, *Science* **2001**, *294*, 1488.
- [38] I. Melngailis, R. H. Rediker, *Proc. IRE* **1962**, *50*, 2428.
- [39] C. S. Roumenin, *Sens. Actuators, A* **1990**, *24*, 83.
- [40] W. Shockley, M. Sparks, G. K. Teal, *Phys. Rev.* **1951**, *83*, 151.
-